EJMI

DOI: 10.14744/ejmi.269269
EJMI 2026;10(3):269–278

Research Article

Interpretable Low-Pass Acoustic Phenotype in COPD From Chest-Wall Breath Sounds: Spectral Anchors and a Target-Aligned MFCC Axis (ModeT)

İhsan Topaloğlu,[1] Çağrı Atasoy,[1] Aylin Bayram,[1] Nil Kuranoğlu,[1] Gülfem Özduygu,[2] Mutlu Onur Güçsav,[3] Abdullah Tanrıkulu,[4] Yekta Bektaş,[5] Arif Metehan Yıldız[6]

[1]Department of Pulmonology, Kafkas University Faculty of Medicine, Kars, Türkiye
[2]Department of Pulmonology, University of Health Sciences, Yedikule Chest Diseases and Thoracic Surgery Training and Research Hospital, Istanbul, Türkiye
[3]Department of Pulmonology, İzmir Bakırçay University, Çiğli Regional Training and Research Hospital, İzmir, Türkiye
[4]Department of Internal Medicine, Siirt Training and Research Hospital, Siirt, Türkiye
[5]Department of Anesthesiology and Reanimation, Kafkas University Faculty of Medicine, Kars, Türkiye
[6]Department of Computer Engineering, Faculty of Engineering, Ardahan University, Ardahan, Türkiye

Abstract

Objectives: High-frequency breath-sound components are attenuated at the chest wall, producing a low-pass effect. We evaluated this pattern across Healthy controls, Stable chronic obstructive pulmonary disease (COPD), and COPD Exacerbation, and assessed whether a mel-frequency cepstral coefficient (MFCC) axis reflected these states.

Methods: We retrospectively analyzed 1,440 posterior recordings from 240 adults (80/group; six 15-s recordings per participant). Spectral bandwidth and 85% spectral roll-off were derived using a short-time Fourier transform pipeline. MFCC1–MFCC13 were summarized by principal component analysis (PCA). ModeT was defined as the PCA component most negatively aligned with both spectral anchors; this rule selected PC6.

Results: Bandwidth differed across groups (210.19, 204.96, 206.89; p=0.002), as did roll-off (303.35, 299.47, 297.89; p=0.013) and ModeT (−0.08, −0.05, 0.14; p=0.001). Ordered trends were significant for all three measures. ModeT explained 3.9% of MFCC variance, correlated with both anchors, and remained higher in Exacerbation than Healthy in clustered record-level models (estimate 0.22, 95% CI 0.09–0.34; p<0.001).

Conclusion: COPD chest-wall recordings show a low-pass spectral shift. Spectral anchors and ModeT define an interpretable acoustic phenotype requiring prospective validation.

Keywords: Chronic obstructive pulmonary disease (COPD); respiratory sound analysis; electronic stethoscope; low-pass acoustic phenotype; mel-frequency cepstral coefficients (MFCC)

Cite This Article: *Topaloğlu İ, Atasoy Ç, Bayram A, Kuranoğlu N, Özduygu G, Güçsav MO, et al. Interpretable Low-Pass Acoustic Phenotype in COPD From Chest-Wall Breath Sounds: Spectral Anchors and a Target-Aligned MFCC Axis (ModeT). EJMI 2026;10(3):269–278.*

Address for correspondence: İhsan Topaloğlu, MD, Department of Pulmonology Kafkas University Faculty of Medicine, Kars, Türkiye
E-mail: ras-topal@hotmail.com

Submitted Date: April 01, 2026 **Revision Date:** July 31, 2026 **Accepted Date:** August 02, 2026

©Copyright 2026 by Eurasian Journal of Medicine and Investigation - Available online at www.ejmi.org
OPEN ACCESS This work is licensed under a Creative Commons Attribution-NonCommercial 4.0 International License.

Chronic obstructive pulmonary disease (COPD) can alter breath sounds recorded at the chest wall. Auscultation remains indispensable at the bedside, yet it is inherently subjective, and inter-listener agreement may be limited, particularly when findings are subtle or mixed.[1] These practical constraints, together with the increasing use of electronic stethoscopes and remote or tele-monitoring, have amplified interest in computerized respiratory sound analysis and more standardized reporting.[2–4]

Breath sounds arise from airflow-related turbulence and flow–structure interactions, then propagate through lung parenchyma and the chest wall before being captured at the body surface.[4,5] This transmission is frequency-dependent, and higher-frequency components are preferentially attenuated, so the chest wall effectively acts as a low-pass filter for respiratory sound energy.[5] A physiologically plausible chest-wall "low-pass signature" would therefore include reduced high-frequency extension and a narrower effective spectrum at the recording site.

Despite its physiological basis, much of the modern literature has focused on machine-learning classification using diverse feature sets and various preprocessing methods, often with limited standardization and less mechanistic insight.[6,7] This highlights the need for complementary approaches that target specific physiological patterns and connect high-dimensional features, like mel-frequency cepstral coefficients (MFCCs), to understandable physiological axes. In this study, we explored whether chest-wall recordings from Stable COPD and COPD Exacerbation show a consistent shift toward a low-pass acoustic phenotype compared with recordings from Healthy controls. We utilized two predefined high-frequency-sensitive spectral markers, Spectral Bandwidth and Spectral Roll-Off, as direct indicators of high-frequency extension. We then identified a single MFCC-space axis (ModeT) by selecting, among the MFCC principal component analysis (PCA) components (PC1–PC13), the one most consistently aligned with these high-frequency (HF) anchors. This approach links MFCC variation to an interpretable HF attenuation axis while maintaining a small, physiologically relevant feature set.

Methods

Study design and ethics

This single-center, cross-sectional retrospective study was conducted at a tertiary care hospital Chest Diseases Clinic. Digitally archived posterior lung sound recordings obtained during routine care between June 1, 2023 and November 30, 2025 were reviewed. The study was reported according to STROBE and all data were analyzed in anonymized form. The protocol complied with the Declaration of Helsinki and was approved by the Kafkas University Clinical Research Ethics Committee (approval no. 80576354-050-99/858; January 28, 2026). Informed consent was waived due to the retrospective, anonymized design. The study and analytical workflow are summarized in Figure 1.

Participants and clinical grouping.

Adults (≥18 years) were eligible if lung sound recordings were technically adequate and corresponding clinical and spirometric data were available. We excluded recordings with insufficient duration, extensive artifacts, missing audio files, major pleural pathology, or acute cardiovascular events at the time of recording. Cases with incomplete clinical or spirometric data were also excluded.

Overall, 240 participants were categorized as Healthy, Stable COPD, or COPD Exacerbation based on clinical status at the time of recording. COPD was confirmed according to

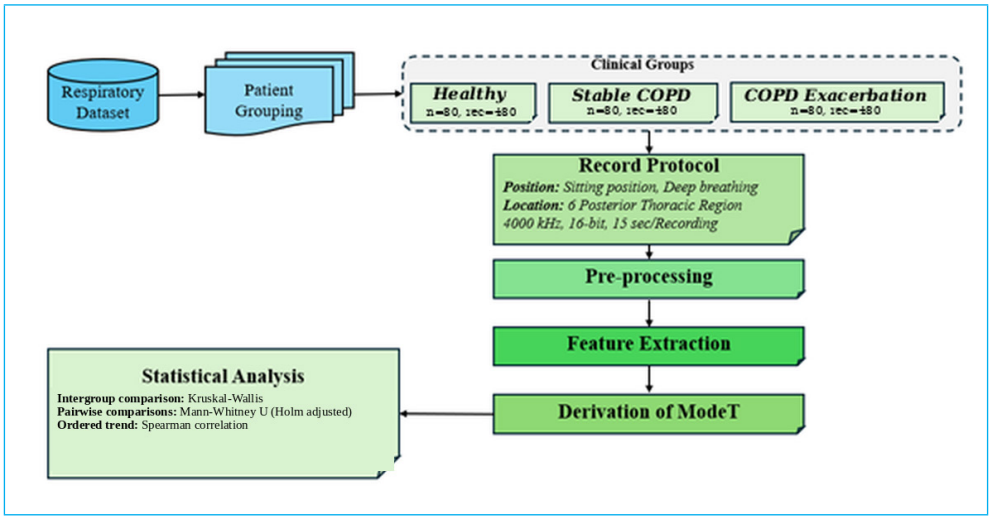

Figure 1. Study and analytical workflow.

the Global Initiative for Chronic Obstructive Lung Disease (GOLD) 2026 criteria.[8] Demographics, smoking exposure (pack-years, where available), comorbidities, clinical findings, spirometry, and CT-reported emphysema status corresponding to the recording date were extracted from the hospital information system.

Healthy participants were identified from archived recordings of individuals who had undergone routine occupational health surveillance at our institution. As these individuals attended for occupational screening rather than respiratory complaints, they represented a population free of known respiratory disease at the time of recording, providing an appropriate reference group for acoustic comparison. Eligible healthy participants were required to have no chronic respiratory symptoms, no known chronic lung disease, no evidence of acute lower respiratory tract infection or pneumonia at the time of recording, and normal spirometry. Chest auscultation was performed by a pulmonologist; the absence of pathological lung sounds was defined as the absence of wheeze, crackles, rhonchi, stridor, or focal/asymmetric reduction in breath sounds. Normal spirometry was defined as post-bronchodilator forced expiratory volume in one second (FEV_1) and forced vital capacity (FVC) ≥80% predicted and FEV_1/FVC ≥0.70.[5,9] Smokers without clinical or spirometric COPD were eligible only if all of these criteria were satisfied.

Stable COPD required post-bronchodilator FEV_1/FVC <0.70 and clinical stability for at least 4 weeks. Stability was defined as no exacerbation, no systemic corticosteroid or antibiotic use, and no change in maintenance inhaler therapy.[9]

COPD exacerbation was defined per GOLD 2026 as an acute worsening of dyspnea and/or cough and sputum requiring additional treatment and typically lasting <14 days.[8,9] Patients on invasive mechanical ventilation were excluded. Technically adequate recordings obtained under supplemental oxygen therapy, or during off periods of intermittent noninvasive ventilation, were included. Patients with COPD exacerbation who were receiving intermittent noninvasive ventilation (NIV) were recorded during a period when NIV was not in use; no recordings were obtained while NIV was actively applied. Because recordings were obtained during routine care, this preserved representativeness of exacerbation physiology, provided the signal showed no overt device or motion artifacts.

Digitally archived posterior thoracic recordings were screened and organized into three group-level datasets (Healthy, Stable COPD, and COPD Exacerbation). Each group included 80 patients and 480 recordings (6 per patient), totaling 240 patients and 1440 recordings. Each 15-s recording was analyzed as a region-specific observation. All patients in the Stable COPD and COPD Exacerbation groups had emphysema reported on a routine chest CT corresponding to the recording period. Emphysema was therefore ascertained qualitatively (present/absent) from radiology reports, and no quantitative densitometric assessment was available.

Recording protocol and quality control

Recordings were obtained in a room with minimized ambient noise using a Littmann CORE digital stethoscope (3M, St. Paul, MN, USA). Participants were seated and instructed to breathe deeply and rhythmically through the mouth. Auscultation was performed at six posterior thoracic sites (bilaterally at the interscapular, mid-scapular, and infrascapular levels). A 15-s recording was obtained from each site and stored at a sampling frequency of 4000 Hz and 16-bit resolution. According to the Nyquist theorem, analyses were restricted to the effective frequency range of 0–2000 Hz.

Segments with prominent artifacts (speech, coughing, patient or stethoscope movement, or contact noise) were excluded based on combined auditory review and visual inspection of waveforms and STFT spectrograms (time–frequency representations). If artifacts affected most of a 15-s segment, the entire segment was discarded. Inspiratory and expiratory phases were not manually separated. All analyses were performed at the recording level and summarized as one value per 15-s segment by taking the median across STFT frames.

Biomarkers were SpectralBW, SpectralRollOff85, MFCC1–MFCC13, and ModeT. Features were computed using a consistent STFT-based pipeline and summarized as a single value per 15-s segment. Primary analyses focused on SpectralBW, SpectralRollOff85, and ModeT as low-dimensional, interpretable markers of spectral spread and high-frequency extension at the chest wall. MFCC1–MFCC13 were assessed exploratorily to characterize spectral-envelope variation beyond the primary markers.

STFT-based spectral and cepstral features (Spectral anchors and MFCCs): definitions and computation

Overview and aggregation to recording level

Spectral and cepstral features were computed per recording using standard short-time Fourier transform (STFT)-based definitions and aggregated to one value per recording (feature-generation pipeline applied consistently across all recordings).

STFT notation (common foundation)

Let $x[n]$ denote the discrete-time signal, $w[n]$ the analysis window, N the fast Fourier transform (FFT) length, H the

hop size, and *fs* the sampling rate. The short-time Fourier transform (STFT) at frame *t* and frequency bin *k* is:

In this study, the STFT was computed using a Hamming analysis window of 25 ms (100 samples at 4000 Hz) with 50% overlap (hop size: 12.5 ms; H = 50 samples). The FFT length was set to N = 512 (frequency resolution: 4000/512 ≈ 7.8 Hz). Power spectra were computed as P_t(k)=|X_t(k)|^2 and restricted to 0–2000 Hz.

$$X_t(k) = \sum_{n=0}^{N-1} x[n + tH]\, w[n]\, e^{-j2\pi kn/N}$$

$$P_t(k) = |X_t(k)|^2, \qquad f_k = k\,\frac{f_s}{N}$$

The spectral centroid is:

$$\mu_t = \frac{\sum_k f_k\, P_t(k)}{\sum_k P_t(k)}$$

Spectral anchors (frame-level definitions)

SpectralBW. SpectralBW summarizes the spread of spectral energy around the spectral centroid and is commonly defined as a p-th order central moment of the magnitude spectrum (often p=2).[10] Lower SpectralBW corresponds to a narrower spectrum and is consistent with reduced HF extension at the chest wall when higher-frequency energy is preferentially attenuated.[3,4,7]

$$BW_t = \left(\frac{\sum_k |f_k - \mu_t|^p\, P_t(k)}{\sum_k P_t(k)}\right)^{1/p}$$

SpectralRollOff85. SpectralRollOff85 is defined as the frequency below which a specified proportion of the total spectral energy is contained; we used the conventional 85% roll-off (r=0.85).[11] Lower SpectralRollOff85 indicates that the energy distribution is concentrated at lower frequencies, consistent with a stronger low-pass signature at the recording site.[4]

$$k_r = \min\left\{k \in \{0,\dots,K\} : \sum_{i=0}^{k} P_t(i) \geq r \sum_{i=0}^{K} P_t(i)\right\}, \qquad RollOff_t = f_{k_r}$$

MFCC representation (STFT-to-mel-to-cepstrum)

Mel-frequency cepstral coefficients (MFCCs) provide a compact description of the spectral envelope in a perceptually motivated (mel) frequency scale. MFCCs are widely used to summarize spectral shape in respiratory sound research; it is common to extract the first 13 coefficients because most energy-related information is concentrated in the lower-order components.[12]

For MFCC extraction, 26 Mel filter banks were applied over 50–2000 Hz. Log-energy compression was performed using the natural logarithm, followed by a type-II discrete cosine transform (DCT). The first 13 coefficients (c0–c12; including c0, reported as MFCC1–MFCC13) were retained. Frame-level MFCCs were summarized to one value per 15-s recording using the median across frames.

The mel frequency mapping is defined as:

$$m(f) = 2595\, log_{10}(1 + \frac{f}{700})$$

Given a mel filterbank $H_m(k)$, m = 1, … ,M, the filterbank energies are:

$$E_m(t) = \sum_k P_t(k)\, H_m(k)\,, \qquad m = 1, \dots, M.$$

Log-energies are computed as:

$$L_m(t) = \log(E_m(t) + \varepsilon)$$

MFCCs are obtained via the DCT-II of log mel energies:

$$c_n(t) = \sum_{m=1}^{M} L_m(t) \cos\left(\frac{\pi n\,(m - 0.5)}{M}\right), \qquad n = 0, \dots, 12$$

In this manuscript, MFCC1–MFCC13 correspond to c0–c12 (i.e., DCT indices 0–12), including c0.

PCA and derivation of ModeT.

We constructed an MFCC feature matrix using MFCC1–MFCC13 and z-scored each coefficient across all recordings (mean=0, standard deviation [SD]=1). PCA was then applied to the standardized MFCC matrix to obtain orthogonal components that capture dominant covariance patterns.[13] We evaluated candidate axes across all MFCC components (PC1–PC13). For each component, we computed its Spearman correlation with each HF anchor (SpectralBW and SpectralRollOff85). ModeT was defined as the component showing the strongest and most consistent alignment with HF attenuation. The sign of the selected component was oriented so that higher ModeT indicates stronger HF attenuation. In this dataset, this selection rule identified the sixth principal component (PC6), which accounted for 3.9% of the total variance of the standardized MFCC matrix; ModeT therefore refers to PC6 throughout. Because ModeT was derived in a data-driven manner within this dataset, it should be considered exploratory and requires external validation.

ModeT (target-aligned MFCC axis).

Let $c_i \in \mathbb{R}^{13}$ denote the recording-level MFCC vector for recording i. Each coefficient is standardized across recordings:

$$z_{ij} = \frac{c_{ij} - \mu_j}{\sigma_j}$$

PCA is applied to the standardized MFCC matrix Z; for component j with loading vector v_j, the component score is:

$$\mathbf{s_{ij}} = \mathbf{z_i^T v_j}$$

For $j \in \{1,...,13\}$, alignment to HF attenuation is quantified by Spearman correlations with the HF anchors:

$$\rho_{j,BW} = \rho_s(s_{\cdot j}, SpectralBW), \quad \rho_{j,RO} = \rho_s(s_{\cdot j}, SpectralRollOff)$$

The ModeT axis is selected as the component with the strongest joint negative alignment:

$$j^* = \arg\min(\rho_{j,BW} + \rho_{j,RO}), \quad j \in \{1,\ldots,13\}$$

The sign is oriented so that higher ModeT indicates stronger HF attenuation:

$$ModeT_i = \begin{cases} s_{ij^*}, & \rho_{j*,BW} + \rho_{j*,RO} < 0 \\ -s_{ij^*}, & \rho_{j*,BW} + \rho_{j*,RO} \geq 0 \end{cases}$$

Statistical Analysis

Signal processing, feature extraction, and PCA-based derivation of ModeT were performed using Python, version 3.11.8 (Python Software Foundation, Wilmington, DE, USA). Statistical analyses were performed using IBM SPSS Statistics for Windows, version 26.0 (IBM Corp., Armonk, NY, USA). Continuous variables were summarized as mean ± SD when approximately normally distributed and as median (interquartile range, IQR) otherwise. Categorical variables were presented as counts and percentages. Group comparisons across Healthy, Stable COPD, and COPD Exacerbation were performed using one-way analysis of variance (ANOVA) for normally distributed variables and the Kruskal–Wallis test for non-normally distributed variables, as appropriate. Chi-square testing was used for categorical variables. For the primary acoustic outcomes (SpectralBW, SpectralRollOff85, and ModeT), significant omnibus results were followed by pairwise post hoc comparisons using the Mann–Whitney U test, with Holm-adjusted p values across the three pairwise contrasts for each measure. Effect sizes for these comparisons are reported as $r = Z/\sqrt{N}$, where Z is the standardized Mann–Whitney statistic and N is the total number of patients in the two groups compared. Ordered change across clinical states was assessed using Spearman's rank correlation coefficient. For the primary patient-level analyses, each participant's value was calculated as the mean of the six posterior site-level recordings. Group summaries are presented as mean ± SD, whereas inferential statistics were based on the tests specified above. Sensitivity analyses were repeated using the median of the six posterior site-level recordings for each participant. In addition, supportive record-level analyses were performed using patient-clustered generalized estimating equations (GEE) to account for within-patient correlation among repeated recordings. Because smoking exposure data were incomplete, smoking was not included as a covariate in the primary models. All statistical tests were two-sided, and $p < 0.05$ was considered statistically significant.

AI-Assisted Technologies Disclosure

The authors used an AI-assisted language tool only to improve grammar, readability, and general language clarity during manuscript preparation. In addition, ChatGPT was used only to assist with figure wording, layout refinement, and visual clarity. The tool was not used to generate scientific content, analyze data, interpret findings, or make scientific decisions. All intellectual content, figure content, data interpretation, and final approval of the manuscript remained the sole responsibility of the authors.

Results

Participant characteristics are summarized in Table 1. Age and body mass index (BMI) differed across groups, while sex distribution was comparable. Emphysema was reported on routine chest CT in all patients in the Stable COPD and COPD Exacerbation groups; chest CT was not performed in the Healthy group. The dataset was balanced across groups, with an identical number of posterior chest-wall recordings per patient.

ModeT showed consistent alignment with spectral anchors based on the selected component (Table 2).

Figure 2a, b show patient-level box plots of SpectralBW and SpectralRollOff85, whereas Figure 2c shows the reported

Table 1. Participant characteristics by group

Variable	Healthy	Stable COPD	COPD Exacerbation	p
Age, years	59.3±10.6	65.1±9.1	64.7±9.6	0.0019
Sex, male/female	56/24	67/12	64/16	0.0693
BMI, kg/m²	22.7±2.1	21.6±2.4	21.5±2.0	0.0019

COPD: Chronic obstructive pulmonary disease; BMI: Body Mass Index.

Table 2. ModeT alignment with spectral anchors

Selected component	Explained variance (%)	ρ with SpectralBW	p (BW)	ρ with SpectralRollOff	p (RollOff)
PC6	3.87	-0.2205	<0.0001	-0.1838	<0.0001

Table 3. Primary patient-level results

Measure	Healthy (mean ± SD)	Stable COPD (mean ± SD)	COPD Exacerbation (mean ± SD)	p	Trend (ρ, p)
SpectralBW	210.1890±11.9690	204.9600±26.9700	206.8860±38.4760	0.0022	-0.2120, 0.0010
SpectralRollOff	303.3540±18.7300	299.4730±43.3320	297.8920±56.9130	0.0129	-0.1851, 0.0040
ModeT	-0.0810±0.2650	-0.0540±0.5570	0.1350±0.4940	0.0010	0.2389, 0.0002

COPD: Chronic obstructive pulmonary disease.

Table 4. Pairwise comparisons

Measure	Comparison	Adjusted p value	Effect size (r)
SpectralBW	Healthy vs COPD Exacerbation	0.0018	0.2719
SpectralBW	Healthy vs Stable COPD	0.0239	0.1988
SpectralBW	Stable COPD vs COPD Exacerbation	0.6709	0.0337
SpectralRollOff	Healthy vs COPD Exacerbation	0.0111	0.2296
SpectralRollOff	Healthy vs Stable COPD	0.0907	0.1584
SpectralRollOff	Stable COPD vs COPD Exacerbation	0.4466	0.0603
ModeT	Healthy vs COPD Exacerbation	0.0003	0.3057
ModeT	Stable COPD vs COPD Exacerbation	0.0892	0.1589
ModeT	Healthy vs Stable COPD	0.1860	0.1047

COPD: Chronic obstructive pulmonary disease.

ModeT group means ± SD. Numerical results and ordered trend statistics are provided in Table 3.

Patient-level group summaries for SpectralBW, SpectralRollOff85, and ModeT are shown in Table 3, with the corresponding visual summaries presented in Figure 2. For the primary analysis, patient-level values were derived as the mean of the six posterior site-level recordings for each participant.

Pairwise group comparisons for the primary measures are shown in Table 4.

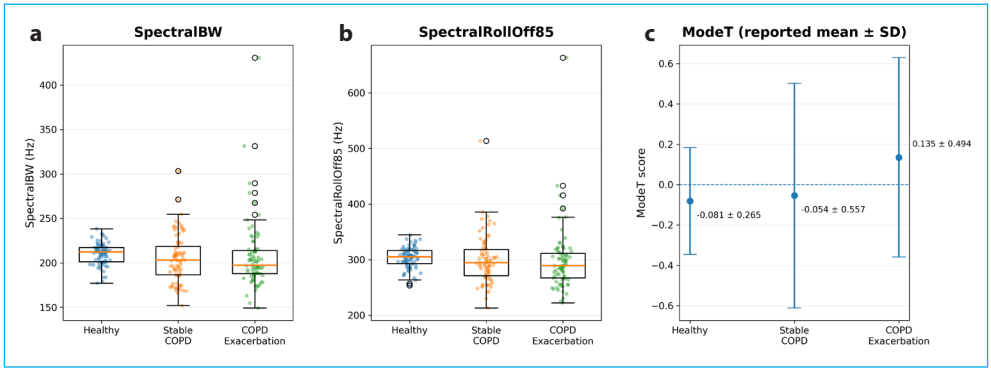

Figure 2. Spectral anchors and ModeT across clinical groups.

(a, b) Patient-level box plots of SpectralBW and SpectralRollOff85. **(c)** Reported ModeT group means ± SD; the dashed line indicates zero.

Table 5. Sensitivity analysis (patient-level medians)

Measure	p	Trend (ρ, p)
SpectralBW	0.0005	-0.2278, 0.0004
SpectralRollOff	0.0145	-0.1811, 0.0049
ModeT	0.0021	0.2265, 0.0004

Sensitivity results using patient-level medians are shown in Table 5 and were directionally consistent with the primary analysis.

Record-level patient-clustered estimates are shown in Table 6.

Discussion

In posterior chest wall breath sound recordings, we observed a low-pass acoustic shift in COPD. The pattern is consistent with reduced high-frequency extension. In the primary patient-level analysis, SpectralBW was lower in both Stable COPD and COPD Exacerbation than in Healthy. SpectralRollOff85 was also lower in COPD Exacerbation than in Healthy, again indicating reduced high-frequency extension at the recording site. In parallel, a target-aligned MFCC axis (ModeT) increased across ordered clinical states and was highest in COPD Exacerbation (Table 3). Pairwise comparisons showed that Healthy differed from COPD Exacerbation for all three measures. However, Stable COPD and COPD Exacerbation did not differ after multiplicity adjustment (Table 4). Although the distributions overlapped, the direction of change was consistent. This supports a group-level spectral phenotype rather than near-perfect separation of individuals.

Several mechanisms may plausibly contribute to this pattern. On the generation side, expiratory airflow limitation reduces regional flow rates, and changes in airway caliber and geometry may shift where turbulence is produced. These processes may also emphasize longer-duration, lower-frequency components of the breath sound envelope. On the transmission side, hyperinflation and structural remodeling may change acoustic impedance. They can also attenuate higher frequencies as sound propagates from intrapulmonary sources to the chest wall. Together, these mechanisms support a coherent low-pass signature at the recording site. The pattern is compatible with obstructive physiology, while remaining agnostic about a single dominant micro-mechanism.[4,7]

The lack of robust separation between Stable COPD and COPD Exacerbation in these low-pass markers suggests that the captured phenotype is dominated by chronic structural components of COPD. It may therefore be less sensitive to short-lived state changes (Table 4). Exacerbations can add transient and spatially heterogeneous phenomena. These include intermittent wheeze, secretion-related sounds, and changes in breathing pattern. Acute treatments may also partially normalize airflow and chest wall transmission. Over short, fixed-duration segments, such acute factors may not shift broad high-frequency extension measures in a systematic way, even when symptoms worsen. Exacerbation is also a heterogeneous clinical construct. Differences in severity, timing relative to therapy, and region- or phase-specific acoustics may dilute consistent broadband shifts at the recording level.

We selected these anchors because they map directly onto the low-pass hypothesis and remain easy to interpret. They are also straightforward to reproduce across cohorts. SpectralBW summarizes how broadly energy spreads around the spectral centroid. SpectralRollOff85 identifies the frequency below which a fixed proportion of total spectral energy is contained. A low-pass shift should therefore narrow bandwidth and move the roll-off boundary downward. As pre-specified low-dimensional descriptors, these anchors also reduce researcher degrees of freedom compared with large feature banks. They provide a physiologically interpretable backbone on which complementary representations, such as MFCCs, can be aligned.[10,11]

Individual MFCC coefficients may differ significantly between groups, but single-coefficient interpretation is challenging. Each MFCC captures a mixture of spectral-en-

Table 6. Record-level patient-clustered estimates

Measure	Contrast	Estimate	95% CI	p
SpectralBW	COPD Exacerbation – Healthy	-3.3034	-12.0779 – 5.4710	0.4606
SpectralBW	Stable COPD – Healthy	-5.2298	-11.6552 – 1.1956	0.1106
SpectralRollOff	COPD Exacerbation – Healthy	-5.4619	-18.5090 – 7.5851	0.4119
SpectralRollOff	Stable COPD – Healthy	-3.8811	-14.1607 – 6.3985	0.4593
ModeT	COPD Exacerbation – Healthy	0.2160	0.0940 – 0.3380	0.0005
ModeT	Stable COPD – Healthy	0.0263	-0.1080 – 0.1606	0.7012

COPD: Chronic obstructive pulmonary disease.

velope properties and can be sensitive to preprocessing choices. Rather than selecting one coefficient post hoc to maximize separation, we applied PCA across MFCC1–MFCC13. We then defined ModeT as the component selected from PC1–PC13 to align with the same physiologic idea as the anchors. The selected component (PC6) explained 3.87% of MFCC variance. It correlated negatively with SpectralBW and SpectralRollOff85 (Spearman rho=-0.2205 and rho=-0.1838, respectively; Table 2). Supporting internal consistency, ModeT increased monotonically across ordered clinical states at the patient level (Table 3). In a record-level support analysis that accounted for within-patient clustering, ModeT also remained higher in COPD Exacerbation than in Healthy (Table 6). This approach preserves a compact summary. At the same time, it keeps the MFCC representation tethered to a clear physiologic pattern.

Respiratory acoustics studies have long described disease-related shifts in spectral shape and high-frequency content. Standardization efforts also emphasize controlling recording conditions and analytic definitions.[3,4,7,14] Reviews of respiratory sound analysis and feature extraction highlight similar concerns. Recording location, phase segmentation, and preprocessing choices can produce divergent findings even when underlying physiology is similar. A recurring barrier to synthesis is that many approaches rely on high-dimensional or model-specific descriptors that are difficult to compare across studies.[6,7,14,15] Our results add to the field by operationalizing a simple physiology-led hypothesis with two transparent anchors. We also provide a principled way to summarize MFCC information through an axis explicitly aligned to those anchors. The framework is designed to be portable. The same anchors can be computed from routine recordings, and the MFCC axis can be re-derived in new cohorts using the same alignment rule. Directly comparable data are scarce, but the available evidence points in the same direction. Using flow-standardised recordings, Malmberg et al.[16] reported a lower median frequency of chest-wall breath sound spectra in COPD than in control subjects, with the clearest separation observed against asthma rather than against health. A systematic review of computerized respiratory sounds in stable COPD likewise concluded that normal respiratory sounds in COPD largely follow the pattern seen in healthy people, and identified small sample sizes and heterogeneous methods as the main limitations of this literature.[17] Our findings extend this work in two respects: the low-pass shift was detectable in a considerably larger cohort using only two transparent spectral anchors, and the same direction of change was reproduced by an independently derived MFCC axis. Conversely, the absence of separation between Stable COPD and COPD Exacerbation is consistent with earlier work comparing computerized respiratory sounds between stable and exacerbated COPD,[18] and suggests that state-level discrimination may require phase- or region-resolved features rather than recording-level summaries.

The observed low-pass shift suggests that a small, interpretable feature set can capture meaningful physiologic information from posterior recordings without complex classifiers. These measures may serve as quantitative descriptors in mechanistic studies that link acoustics to airflow limitation, hyperinflation, or imaging phenotypes. They may also help standardize comparisons across recording systems by focusing on a defined pattern rather than a model-dependent label. Because overlap between groups is substantial, these markers should be interpreted as phenotypic descriptors. They may be better suited as endpoints for longitudinal change than as stand-alone diagnostic tests.

Conclusion

Using two transparent HF spectral anchors and a target-aligned MFCC axis, we demonstrate a reproducible low-pass spectral shift in routine posterior chest-wall recordings from COPD compared with Healthy recordings. The convergence of anchors and ModeT supports a coherent, interpretable acoustic phenotype that is suitable for replication and for mechanistic linkage to physiologic and imaging markers in future studies.

Limitations

Group differences in age and BMI may have influenced breathing mechanics and chest wall sound transmission. Smoking exposure data were incomplete and could not be incorporated into the primary adjusted analyses. Recordings obtained during COPD exacerbation may have included supplemental oxygen, and some patients were receiving intermittent noninvasive ventilation. Although invasive ventilation was excluded and all recordings were obtained during noninvasive ventilation-free intervals, carry-over effects of recent positive-pressure support on breathing pattern, together with supplemental oxygen, can alter acoustic spectra and may contribute to residual confounding. Larger cohorts are needed to confirm these findings with covariate-adjusted analyses. Emphysema was ascertained qualitatively from routine radiology reports rather than by quantitative computed tomography densitometry, so emphysema severity and phenotype could not be related to the acoustic measures. Recordings were obtained from routine posterior sites and were analyzed without phase-specific segmentation. As a result, inspiration- and

expiration-specific features were not examined. Region-resolved analyses may also reveal additional state-dependent information, particularly during exacerbations. Using a single recording system supports internal consistency. However, device frequency response and software implementations can affect absolute spectral estimates. Replication across different hardware and processing pipelines is therefore required. Finally, we did not validate these acoustic markers against spirometric severity or quantitative imaging beyond group status. Future work should link the markers to airflow obstruction, symptom burden, and quantitative CT phenotypes to strengthen mechanistic interpretation and clinical translation.

Highlights

- Posterior chest-wall breath sounds showed a consistent low-pass spectral shift in COPD compared with Healthy.
- Using two transparent high-frequency anchors and a target-aligned MFCC axis (ModeT), we summarize an interpretable group-level acoustic phenotype across Healthy, Stable COPD, and COPD Exacerbation.
- These descriptors are reproducible and may support cross-cohort standardization and future linkage to spirometry and quantitative computed tomography (CT); they are not intended as stand-alone diagnostic tests.

Disclosure

Ethics Committee Approval: The study was conducted in accordance with the Declaration of Helsinki and was approved by the Kafkas University Clinical Research Ethics Committee (approval no. 80576354-050-99/858; January 28, 2026).

Informed Consent: The requirement for informed consent was waived because of the retrospective, anonymized design.

Conflict of Interest: The authors declare no conflict of interest.

Funding: No funding was received for this study.

Use of AI for Writing Assistance: The authors used an AI-assisted language tool only to improve grammar, readability, and general language clarity during manuscript preparation. In addition, ChatGPT was used only to assist with figure wording, layout refinement, and visual clarity. The tool was not used to generate scientific content, analyze data, interpret findings, or make scientific decisions. All intellectual content, figure content, data interpretation, and final approval of the manuscript remained the sole responsibility of the authors.

Author Contributions: Concept: İT, ÇA, AMY; Design: İT, ÇA, AMY, YB; Supervision: İT, ÇA; Materials: İT, ÇA, AB, NK, GÖ, MOG, AT, YB; Data Collection and/or Processing: İT, ÇA, AB, NK, GÖ, MOG, AT, YB; Analysis and/or Interpretation: İT, AMY, ÇA; Literature Review: İT, ÇA, AB, NK; Writing: İT, AMY, ÇA; Critical Review: İT, ÇA, AB, NK, GÖ, MOG, AT, YB, AMY.

Peer-review: Externally peer-reviewed.

References

1. Aviles-Solis JC, Vanbelle S, Halvorsen PA, Francis N, Cals JWL, Andreeva EA, et al. International perception of lung sounds: a comparison of classification across some European borders. BMJ Open Respir Res 2017;4(1):e000250. [CrossRef]
2. Hirosawa T, Harada Y, Ikenoya K, Kakimoto S, Aizawa Y, Shimizu T. The utility of real-time remote auscultation using a Bluetooth-connected electronic stethoscope: open-label randomized controlled pilot trial. JMIR Mhealth Uhealth 2021;9(7):e23109. [CrossRef]
3. Sovijärvi ARA, Vanderschoot J, Earis JE. Standardization of computerized respiratory sound analysis. Eur Respir Rev 2000;10:585–90.
4. Pasterkamp H, Kraman SS, Wodicka GR. Respiratory sounds: advances beyond the stethoscope. Am J Respir Crit Care Med 1997;156(3 Pt 1):974–87. [CrossRef]
5. Sarkar M, Madabhavi I, Niranjan N, Dogra M. Auscultation of the respiratory system. Ann Thorac Med 2015;10(3):158–68. [CrossRef]
6. Pramono RXA, Bowyer S, Rodriguez-Villegas E. Automatic adventitious respiratory sound analysis: a systematic review. PLoS One 2017;12:e0177926. [CrossRef]
7. Reichert S, Gass R, Brandt C, Andrès E. Analysis of respiratory sounds: state of the art. Clin Med Circ Respirat Pulm Med 2008;2:45–58. [CrossRef]
8. Global Initiative for Chronic Obstructive Lung Disease (GOLD). Global Strategy for the Prevention, Diagnosis and Management of COPD: 2026 Report. 2026. Available at: https://goldcopd.org/2026-gold-report-and-pocket-guide/ Accessed on Jan 9, 2026.
9. Pellegrino R, Viegi G, Brusasco V, Crapo RO, Burgos F, Casaburi R, et al. Interpretative strategies for lung function tests. Eur Respir J 2005;26(5):948–68. [CrossRef]
10. Peeters G. A large set of audio features for sound description (similarity and classification). IRCAM Technical Report. 2004. Available online: https://www.ircam.fr/media/uploads/documents/peeters_2004.pdf Accessed on January 9, 2026.
11. Tzanetakis G, Cook P. Musical genre classification of audio signals. IEEE Trans Speech Audio Process 2002;10(5):293–302. [CrossRef]
12. Davis SB, Mermelstein P. Comparison of parametric representations for monosyllabic word recognition in continuously spoken sentences. IEEE Trans Acoust Speech Signal Process 1980;28(4):357–66. [CrossRef]
13. Jolliffe IT, Cadima J. Principal component analysis: a review and recent developments. Philos Trans A Math Phys Eng Sci 2016;374(2065):20150202. [CrossRef]
14. Alías F, Socoró JC, Sevillano X. A review of physical and perceptual feature extraction techniques for speech, music and environmental sounds. Appl Sci (Basel) 2016;6(5):143. [CrossRef]

15. Rocha BM, Pessoa D, Marques A, Carvalho P, Paiva RP. Automatic classification of adventitious respiratory sounds: a (un)solved problem? Sensors (Basel) 2020;21(1):57. [CrossRef]
16. Malmberg LP, Pesu L, Sovijärvi ARA. Significant differences in flow standardised breath sound spectra in patients with chronic obstructive pulmonary disease, stable asthma, and healthy lungs. Thorax 1995;50(12):1285–91. [CrossRef]
17. Jácome C, Marques A. Computerized respiratory sounds in patients with COPD: a systematic review. COPD 2015;12(1):104–12. [CrossRef]
18. Jácome C, Oliveira A, Marques A. Computerized respiratory sounds: a comparison between patients with stable and exacerbated COPD. Clin Respir J 2017;11(5):612–20. [CrossRef]